Effects of particle-hole excitations to nuclear Schiff moments in Xe isotopes

E. Teruya,[1,*] N. Yoshinaga,[1,†] K. Higashiyama,[2,‡] and K. Asahi[3]
[1]*Department of Physics, Saitama University, Saitama City 338-8570, Japan*
[2]*Department of Physics, Chiba Institute of Technology, Narashino, Chiba 275-0023, Japan*
[3]*Department of Physics, Tokyo Institute of Technology, 2-12-1 Oh-okayama, Meguro-ku, Tokyo 152-8551, Japan*
(Received 12 August 2016; revised manuscript received 8 April 2017; published 12 July 2017)

The existence of the permanent electric dipole moment of a fundamental particle implies violation of time reversal invariance. The electric dipole moment of a diamagnetic neutral atom is mainly induced by the nuclear Schiff moment. In this study the Schiff moments induced by the interaction which violates parity and time reversal invariance are calculated for various Xe isotopes using the shell-model wave functions. The contributions to the Schiff moment from one-particle and one-hole excitations turn out to be very different from orbital to orbital. It is also found that the contributions from the core excitations are larger than other particle-hole contributions.

DOI: 10.1103/PhysRevC.96.015501

I. INTRODUCTION

The electric dipole moment (EDM) is a physical observable which violates time reversal symmetry. Through the CPT theorem stating that the simultaneous application of charge (C), parity (P), and time (T) reversal operators keeps the total symmetry of a system, violation of T reversal symmetry is equivalent to the violation of CP reversal symmetry. The Standard Model in particle physics violates CP invariance only through a single phase in the Kobayashi-Maskawa matrix that mixes quark flavors [1]. The resulting T reversal violation is therefore expected to produce only tiny EDMs.

At present the upper limit on the neutron EDM is experimentally $2.9 \times 10^{-26} e$ cm [2]. However, the Standard Model predicts quite a small value, $10^{-32} e$ cm [3–5]. Some theories beyond the Standard Model predict larger EDMs [5–8]. Thus if an EDM is observed experimentally to be larger than those predicted by the Standard Model, it would provide evidence for physics beyond the Standard Model, and also places important constraints on the construction of a new physics.

EDMs originating from CP violation in the hadron sector are searched for in neutron and diamagnetic atoms such as ^{129}Xe, ^{199}Hg, and ^{225}Ra. Measurements of EDMs for these atoms have been attempted and their upper limits are $4.1 \times 10^{-27} e$ cm for ^{129}Xe [9], $7.4 \times 10^{-30} e$ cm for ^{199}Hg [10], and $5.0 \times 10^{-22} e$ cm for ^{225}Ra [11]. At present with new techniques, experimental efforts searching for EDMs of diamagnetic atoms are now in progress [12–15]. Hadronic CP violation may also be searched for in ions [16]. It was theoretically reported that the nuclear EDM would be measured directly by using an ion instead of a neutral atom [17,18]. The EDM of ^{6}Li ion was calculated assuming the one-meson exchange P and T violating nuclear forces recently [19].

The EDM of a neutral diamagnetic atom arises from the Schiff moment of the nucleus. The nuclear Schiff moment originates mainly from two different sources; from nucleon intrinsic EDMs, and from the two-body nuclear interaction which violates P and T invariance. In the latter case theoretical calculations have been carried out for Hg, Rn, and Ra isotopes using mean field theories [20–25]. However, until recently not so many nuclei have been investigated theoretically.

In our previous study [26], the EDMs and Schiff moments of Xe, Ba, and Ce isotopes arising from the nucleon intrinsic EDMs were calculated in terms of the nuclear shell model. The EDMs and Schiff moments of Xe isotopes which come from interactions violating P and T invariance were also calculated [27,28].

In the present paper the Schiff moments of the lowest $1/2^+$ states for ^{135}Xe, ^{133}Xe, ^{131}Xe, and ^{129}Xe nuclei are calculated assuming two-body interactions violating P and T invariance. Particularly effects of the particle-hole excitations from the core of the nucleus are considered, which were not considered in our previous study [27]. Furthermore, contributions to the Schiff moment from one orbital to another is individually calculated and analyzed.

The paper is organized as follows. In Sec. II, the framework of the nuclear Schiff moments and the method of calculations are presented. In Sec. III numerical results are given for the Schiff moments. In Sec. IV the detailed discussion is performed. Finally the results are summarized in Sec. V.

II. THEORETICAL FRAMEWORK

The Schiff moment operator $\boldsymbol{S}$ coming from the asymmetric charge distribution in a nucleus [29] is expressed in terms of spherical tensors

$$S_{\mu}^{(1)} = \sum_{i=1}^{A} \frac{e_i}{10}\left(r_i^2 r_{i,\mu}^{(1)} - \frac{5}{3}\langle r^2\rangle_{\rm ch} r_{i,\mu}^{(1)} + \frac{\sqrt{10}}{3}\left[Q_i^{(2)} \otimes r_i^{(1)}\right]_{\mu}^{(1)}\right) \tag{1}$$

with

$$r_{i,\mu}^{(1)} = r_i C_{\mu}^{(1)}(\theta_i,\varphi_i), \tag{2}$$

$$Q_{i,\mu}^{(2)} = 2 r_i^2 C_{\mu}^{(2)}(\theta_i,\varphi_i), \tag{3}$$

*teruya@nuclei.th.phy.saitama-u.ac.jp
†yoshinaga@phy.saitama-u.ac.jp
‡koji.higashiyama@it-chiba.ac.jp

where $C_\mu^{(L)}$ represents the unnormalized spherical harmonics with rank L and its projection μ, and i represents the ith nucleon. Here A is the mass number of a specific nucleus, and $\boldsymbol{r}_i = (r_i,\theta_i,\varphi_i)$ indicates ith nucleon position. In this study the Schiff moments are calculated for the lowest states with spin $I = 1/2$. The third term in Eq. (1) vanishes for these states since there is no quadrupole moment for $I = 1/2$ states. Here e_i is the charge for the ith nucleon. $e_i = e$ is taken for a proton and $e_i = 0$ is assumed for a neutron. The $\langle r^2\rangle_{\rm ch}$ is the mean squared radius of the nuclear charge distribution [27].

By perturbation theory, the expectation value of the Schiff moment operator is expressed as

$$S = \sum_{T=0,1,2} S_{(T)}, \tag{4}$$

$$S_{(T)} = \sum_k \frac{\langle I_1^+|S_0^{(1)}|I_k^-\rangle\langle I_k^-|V_{\pi(T)}^{PT}|I_1^+\rangle}{E_1^+ - \langle I_k^-|H_0|I_k^-\rangle} + \text{c.c.}, \tag{5}$$

where $V_{\pi(T)}^{PT}$ represents the isoscalar ($T = 0$), isovector ($T = 1$), or isotensor ($T = 2$) interactions between nucleons. Here, $|I_1^+\rangle$ and E_1^+ represent the wave function and the eigenenergy of the lowest state with spin I and positive parity for the Hamiltonian H_0, respectively. $|I_k^-\rangle$ represents the kth intermediate state with spin I and negative parity. Note that this expression is valid as long as $|I_k^-\rangle$ forms an orthonormal complete system and each state $|I_k^-\rangle$ is not necessary to be the eigenstate of the Hamiltonian H_0. The details of this equation are given in Appendix A. In the present study, only $I = 1/2$ states are considered. All these states have their projection (spin third component) $+1/2$.

The lowest positive parity state, $|I_1^+\rangle$, is calculated using the pair-truncated shell model (PTSM) [33–35]. The PTSM is one of the shell-model approaches, but a gigantic shell model space is restricted to the space mainly made of only low-spin collective pairs. For single particle energies, five orbitals between magic numbers 50 and 82 ($0g_{7/2}$, $1d_{3/2}$, $1d_{5/2}$, $2s_{1/2}$, and $0h_{11/2}$) are taken for neutrons and protons. The details of the framework and Hamiltonian for diagonalization are given in Ref. [35].

In this paper the P and T violating two-body interactions $V_{\pi(T)}^{PT}$ in Eq. (5) are considered as follows, which are explicitly written as [30–32]:

$$V_{\pi(0)}^{PT} = F_0(\boldsymbol{\tau}_1\cdot\boldsymbol{\tau}_2)(\boldsymbol{\sigma}_1-\boldsymbol{\sigma}_2)\cdot\boldsymbol{r}\,f(r), \tag{6}$$

$$V_{\pi(1)}^{PT} = F_1[(\tau_{1z}+\tau_{2z})(\boldsymbol{\sigma}_1-\boldsymbol{\sigma}_2) + (\tau_{1z}-\tau_{2z})(\boldsymbol{\sigma}_1+\boldsymbol{\sigma}_2)]\cdot\boldsymbol{r}\,f(r), \tag{7}$$

$$V_{\pi(2)}^{PT} = F_2(3\tau_{1z}\tau_{2z}-\boldsymbol{\tau}_1\cdot\boldsymbol{\tau}_2)(\boldsymbol{\sigma}_1-\boldsymbol{\sigma}_2)\cdot\boldsymbol{r}\,f(r), \tag{8}$$

where

$$f(r) = \frac{\exp(-m_\pi r)}{m_\pi r^2}\left(1+\frac{1}{m_\pi r}\right) \tag{9}$$

with $\boldsymbol{r} = \boldsymbol{r}_1 - \boldsymbol{r}_2$, and $r = |\boldsymbol{r}|$. The coefficients F_T ($T = 0,1,2$) are expressed as

$$F_0 = -\frac{1}{8\pi}\frac{m_\pi^2}{M_N}\bar{g}_{\pi NN}^{(0)}g_{\pi NN}, \tag{10}$$

$$F_1 = -\frac{1}{16\pi}\frac{m_\pi^2}{M_N}\bar{g}_{\pi NN}^{(1)}g_{\pi NN}, \tag{11}$$

$$F_2 = -\frac{1}{8\pi}\frac{m_\pi^2}{M_N}\bar{g}_{\pi NN}^{(2)}g_{\pi NN}, \tag{12}$$

where M_N is mass of a nucleon, m_π is mass of a pion, and $g_{\pi NN}$ is the strong πNN coupling constant, and $\bar{g}_{\pi NN}^{(T)}$ is the strong πNN constant which violates P and T invariance with isospin T. In the following $\bar{g}_{\pi NN}^{(T)}$ and $g_{\pi NN}$ are denoted as $\bar{g}^{(T)}$ and g for short, respectively.

The total Schiff moment is the summation of three isospin components. In this study, Schiff moments are evaluated as coefficients in front of $\bar{g}^{(T)}g$,

$$S = a_{(0)}\bar{g}^{(0)}g + a_{(1)}\bar{g}^{(1)}g + a_{(2)}\bar{g}^{(2)}g. \tag{13}$$

Any intermediate state $|I_k^-\rangle$ in Eq. (5) is represented as a one-particle and one-hole excited state ($1p1h$-state) from the $|I_1^+\rangle$ state. Since the Schiff moment operator is a one-body operator working only on protons, it is enough to consider proton excited $1p1h$ states. To evaluate the Schiff moment in Eq. (5), kth intermediate $1p1h$ state is given as

$$|I_k^-\rangle = |(ij)K;I^-\rangle = N_{ij}^{(K)}[[c_{i\pi}^\dagger \tilde{c}_{j\pi}]^{(K)} \otimes |I_1^+\rangle]^{(I)}, \tag{14}$$

where $c_{i\pi}^\dagger$ ($c_{j\pi}$) represents the proton creation (annihilation) operator in the orbital i (j), with $\tilde{c}_{jm} = (-1)^{j-m}c_{j-m}$. Namely, a $1p1h$ state with spin K, in which one proton excites from orbital j to orbital i by the Schiff moment operator, is coupled with the lowest state $|I_1^+\rangle$ to form an excited state $|I_k^-\rangle$. $N_{ij}^{(K)}$ is a normalization constant determined as $\langle I_k^-|I_k^-\rangle = 1$. Here K can take 1 or 0 for $I = 1/2$. The details of the orthogonalization method are given in Appendix C.

By neglecting the residual interaction, the energy denominator in Eq. (5) is approximately treated as $E_1^+ - \langle I_k^-|H_0|I_k^-\rangle \sim (-E_{ij})$, where $E_{ij} \equiv \varepsilon_i - \varepsilon_j$ represents the single particle-hole excitation energies from orbital j to i. Then Eq. (5) is written as

$$S_{(T)} = -\sum_{Kij} \frac{\langle I_1^+|S_0^{(1)}|I_k^-\rangle\langle I_k^-|V_{\pi(T)}^{PT}|I_1^+\rangle}{E_{ij}} + \text{c.c.} \tag{15}$$

The details of this approximation are explained in Appendix B and the validity of this approximation is discussed in Sec. IV.

To calculate Eq. (15), three types of $1p1h$ excitations are considered. The first type is a set of excitations from an orbital between 50 and 82 to an orbital over 82. These excitations are called type-I excitations. The second type is a set of excitations from an orbital under 50 to an orbital between 50 and 82. These excitations are called type-II excitations. The third type is a set of excitations from an orbital under 50 to an orbital over 82. These excitations are called type-III excitations. Note that excitations among orbitals between 50 and 82 have no contributions since these orbitals are not connected by the

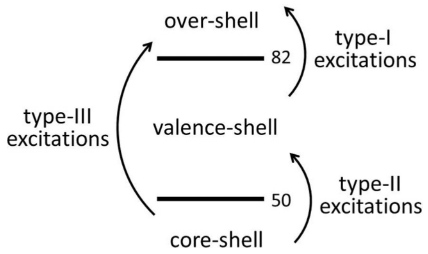

FIG. 1. The schematic illustration of three types of $1p1h$ excitations considered in this study.

Schiff moment operator. The schematic picture representing three types of $1p1h$ excitations is shown in Fig. 1.

For the type-I excitation, an intermediate state is explicitly written as

$$|I_k^-\rangle_{\text{type-I}} = N_{ph}^{(K)}[[a_{p\pi}^\dagger \tilde{c}_{h\pi}]^{(K)} \otimes |I_1^+\rangle]^{(I)}. \tag{16}$$

Here $a_{p\pi}^\dagger$ represents the proton creation operator in the orbital p, where p indicates an orbital over 82. $\tilde{c}_{h\pi}$ represents the proton annihilation operator in the orbital h, where h indicates an orbital between 50 and 82. For the type-II excitation, an intermediate state is written as

$$|I_k^-\rangle_{\text{type-II}} = N_{ph}^{(K)}[[c_{p\pi}^\dagger \tilde{b}_{h\pi}]^{(K)} \otimes |I_1^+\rangle]^{(I)}. \tag{17}$$

Here, $c_{p\pi}^\dagger$ represents the proton creation operator in an orbital p, where p indicates an orbital between 50 and 82. $\tilde{b}_{h\pi}$ represents the proton annihilation operator in the orbital h, where h indicates an orbital under 50. For the type-III excitation, an intermediate state is written as

$$|I_k^-\rangle_{\text{type-III}} = N_{ph}^{(K)}[[a_{p\pi}^\dagger \tilde{b}_{h\pi}]^{(K)} \otimes |I_1^+\rangle]^{(I)}. \tag{18}$$

In this study, all orbitals under the magic number 50 are considered for core orbitals. However, $0d_{3/2}$, $1s_{1/2}$, and $0s_{1/2}$ orbitals are not connected by the Schiff moment operator. For orbitals over the magic number 82, all orbitals up to the primary quantum number $N = 8\hbar\omega$ from the bottom are considered. However, $2d_{5/2}$, $0j_{15/2}$, $0j_{13/2}$, $1h_{11/2}$, $0k_{15/2}$, $0k_{17/2}$, $2g_{7/2}$, $3d_{3/2}$, $3d_{5/2}$, and $4s_{1/2}$ orbitals are also not connected by the Schiff moment operator. Orbitals over 8 $\hbar\omega$ have no contributions to the Schiff moment. This is because the Schiff moment operator in Eq. (1) is constructed from the $\langle r_i^2 \mathbf{r}_i\rangle$ and $\langle r_i^2\rangle\langle \mathbf{r}_i\rangle$, and the following constraints are imposed: $|\Delta n| \leqslant 3$, $|\Delta\ell| = 1{,}3$, and $|\Delta j| \leqslant 1$, where n, ℓ, and j indicate the radial oscillator quantum number, the orbital angular momentum, and the total spin angular momentum, respectively.

The energy of each single particle orbital is taken from the Nilsson energy [36] as

$$\varepsilon_{n\ell j} = \left(2n + \ell + \tfrac{3}{2}\right)\hbar\omega - \kappa(2\boldsymbol{\ell}\cdot\mathbf{s} + \mu(\boldsymbol{\ell}^2 - \langle\boldsymbol{\ell}^2\rangle_N))\hbar\omega \tag{19}$$

with $\kappa = 0.0637$ and $\mu = 0.60$, where $\langle\boldsymbol{\ell}^2\rangle_N = \frac{1}{2}N(N+3)$ and $\hbar\omega = 41A^{-1/3}$ MeV. The schematic figure representing the single particle orbitals considered in this study for ^{129}Xe is shown in Fig. 2.

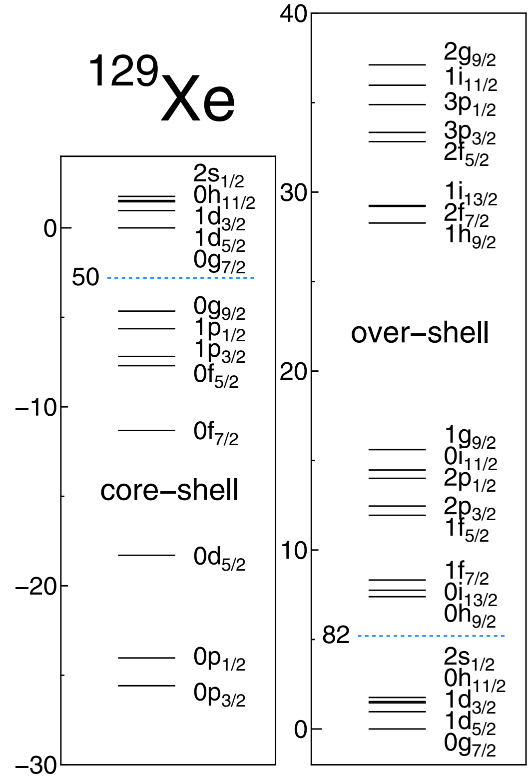

FIG. 2. The proton-single-particle energy for each orbital taken for ^{129}Xe in units of MeV. The energy of the $0g_{7/2}$ orbital is adjusted to be zero. Orbitals which are not connected by the Schiff moment operator are not shown.

III. NUMERICAL RESULTS

To analyze the contribution to the Schiff moments from each orbital, firstly a partial contribution of the excitation from any orbital (h) between 50 and 82 to a specific orbital (p) over 82 (type-I excitations) is defined as

$$s_{(T)}^{\text{type-I}}(p) = -\sum_{Kh} \frac{\langle I_1^+|S_0^{(1)}|I_k^-\rangle\langle I_k^-|V_{\pi(T)}^{PT}|I_1^+\rangle}{E_{ph}} + \text{c.c.}, \tag{20}$$

which is rewritten in terms of $\bar{g}^{(T)}g$ as

$$s_{(T)}^{\text{type-I}}(p) = a_{(T)}^{\text{type-I}}(p)\bar{g}^{(T)}g, \tag{21}$$

where and $a_{(T)}^{\text{type-I}}(p)$'s are coefficients so determined in evaluating the partial Schiff moment $s_{(T)}^{\text{type-I}}(p)$.

Secondly, a partial contribution of the excitation to any orbital (p) between 50 and 82 from a specific orbital (h) under 50 (type-II excitations) is defined as

$$s_{(T)}^{\text{type-II}}(h) = -\sum_{Kp} \frac{\langle I_1^+|S_0^{(1)}|I_k^-\rangle\langle I_k^-|V_{\pi(T)}^{PT}|I_1^+\rangle}{E_{ph}} + \text{c.c.}, \tag{22}$$

which is rewritten in terms of $\bar{g}^{(T)}g$ as

$$s_{(T)}^{\text{type-II}}(h) = a_{(T)}^{\text{type-II}}(h)\bar{g}^{(T)}g. \tag{23}$$

TABLE I. Calculated results of $a_{(T)}^{\text{type-I}}(p)$ from each orbital p in the shell over 82 (type-I excitations) for ^{129}Xe (in units of 10^{-3} $e$fm^3).

T	$1f_{7/2}$	$0h_{9/2}$	$0i_{13/2}$	$2p_{3/2}$
0	+0.107	+0.265	−0.007	+0.079
1	+0.047	+0.107	−0.005	+0.049
2	+0.176	+0.380	−0.025	+0.214
T	$1f_{5/2}$	$1p_{1/2}$	$1g_{9/2}$	$0i_{11/2}$
0	+0.385	+0.055	+0.018	+0.001
1	+0.153	+0.020	+0.008	+0.000
2	+0.531	+0.063	+0.027	+0.000
T	$1h_{9/2}$	$2f_{5/2}$	$2f_{7/2}$	$3p_{1/2}$
0	+0.406	−0.062	+0.076	−0.013
1	+0.184	−0.025	+0.050	−0.001
2	+0.699	−0.089	+0.222	+0.007
T	$3p_{3/2}$	$1i_{11/2}$	$1i_{13/2}$	$2g_{9/2}$
0	+0.002	+0.000	+0.010	−0.001
1	−0.007	+0.000	+0.007	−0.000
2	−0.045	+0.000	+0.032	−0.001

Finally, a partial contribution of the excitation from a specific orbital (h) under 50 to any orbital (p) over 82 (type-III excitations) is also defined as

$$s_{(T)}^{\text{type-III}}(h) = -\sum_{Kp} \frac{\langle I_1^+|S_0^{(1)}|I_k^-\rangle\langle I_k^-|V_{\pi(T)}^{PT}|I_1^+\rangle}{E_{ph}} + \text{c.c.}, \tag{24}$$

which is rewritten in terms of $\bar{g}^{(T)}g$ as

$$s_{(T)}^{\text{type-III}}(h) = a_{(T)}^{\text{type-III}}(h)\bar{g}^{(T)}g, \tag{25}$$

Table I shows calculated $a_{(T)}^{\text{type-I}}(p)$ for ^{129}Xe. The contributions from the $1f_{7/2}$, $0h_{9/2}$, $1f_{5/2}$, and $1h_{9/2}$ orbitals are large since those orbitals in the 50–82 major shell mostly contribute positively. Table II shows calculated $a_{(T)}^{\text{type-II}}(h)$ for ^{129}Xe. The contribution from the $0g_{9/2}$ orbital becomes the largest. The $0g_{9/2}$ orbital is connected to the $0h_{11/2}$ orbital by the Schiff moment operator. The orbitals which demand large $1p1h$-excitation energies (like $0p_{3/2}$ and $0p_{1/2}$ orbitals) also have considerable contributions. Table III shows calculated $a_{(T)}^{\text{type-III}}(h)$ for ^{129}Xe. These contributions are not so large compared to results in Table II.

TABLE II. Calculated results of $a_{(T)}^{\text{type-II}}(h)$ from each orbital h in the shell under 50 (type-II excitations) for ^{129}Xe (in units of 10^{-3} $e$fm^3).

T	$0g_{9/2}$	$1p_{1/2}$	$0f_{5/2}$	$1p_{3/2}$
0	−3.642	+0.621	+1.964	+1.443
1	−2.022	+0.511	+0.867	+0.502
2	−8.488	+2.444	+3.239	+1.568
T	$0f_{7/2}$	$0p_{1/2}$	$0p_{3/2}$	
0	+0.883	+0.648	+0.982	
2	+0.473	+0.273	+0.536	
3	+1.953	+0.988	+2.236	

TABLE III. Calculated results of $a_{(T)}^{\text{type-III}}(h)$ from each orbital h in the shell under 50 (type-III excitations) for ^{129}Xe (in units of 10^{-3} $e$fm^3).

T	$0g_{9/2}$	$1p_{1/2}$	$0f_{5/2}$	$1p_{3/2}$
0	−0.090	−0.134	−0.008	−0.336
1	+0.007	+0.060	−0.028	−0.146
2	+0.134	+0.491	−0.015	−0.537
T	$0f_{7/2}$	$0d_{3/2}$	$1s_{1/2}$	$0d_{5/2}$
0	−0.029	+0.055	−0.416	−0.036
1	−0.018	+0.020	−0.389	−0.028
2	−0.076	+0.064	−1.918	−0.133

Table IV shows the calculated results of $a_{(T)}$ for the lowest $I = 1/2$ states of Xe isotopes. Here, using Eqs. (21), (23), and (25), $a_{(T)}$ is given by

$$a_{(T)} = a_{(T)}^{\text{type-I}} + a_{(T)}^{\text{type-II}} + a_{(T)}^{\text{type-III}} \tag{26}$$

with

$$a_{(T)}^{\text{type-I}} = \sum_p a_{(T)}^{\text{type-I}}(p), \tag{27}$$

$$a_{(T)}^{\text{type-II}} = \sum_h a_{(T)}^{\text{type-II}}(h), \tag{28}$$

$$a_{(T)}^{\text{type-III}} = \sum_h a_{(T)}^{\text{type-III}}(h). \tag{29}$$

The contributions of the core excitations are a few times larger than those from the over-shell excitations for most of the isospin components. The isotensor ($T = 2$) components are largest for all nuclei. The previous results [27] are also shown in Table IV. By comparing the present results with the previous ones, some contributions of Schiff moments are found to be nearly one order of magnitude larger than the previous ones (for examples, isotensor components of ^{135}Xe and ^{133}Xe). The

TABLE IV. Calculated results of $a_{(T)}$ for the lowest $1/2^+$ states (in units of 10^{-3} $e$fm^3). Previous results ($a_{(T)}^{\text{prev}}$) are taken from Ref. [27].

	T	$a_{(T)}^{\text{type-I}}$	$a_{(T)}^{\text{type-II}}$	$a_{(T)}^{\text{type-III}}$	$a_{(T)}$	$a_{(T)}^{\text{prev}}$
^{135}Xe	0	+2.357	+0.670	−1.057	+1.969	+0.630
	1	+1.297	+1.693	−0.602	+2.389	+0.323
	2	+5.427	+9.490	−2.554	+12.363	+1.31
^{133}Xe	0	+1.812	+1.716	−1.047	+2.481	+0.464
	1	+0.949	+1.510	−0.578	+1.882	+0.285
	2	+3.982	+7.343	−2.419	+8.906	+1.24
^{131}Xe	0	+1.575	+2.097	−0.968	+2.704	+0.514
	1	+0.787	+1.282	−0.530	+1.539	+0.352
	2	+3.145	+5.596	−2.177	+6.564	+1.60
^{129}Xe	0	+1.322	+2.897	−0.978	+3.242	+0.507
	1	+0.586	+1.140	−0.522	+1.204	+0.399
	2	+2.192	+3.940	−1.961	+4.172	+1.89

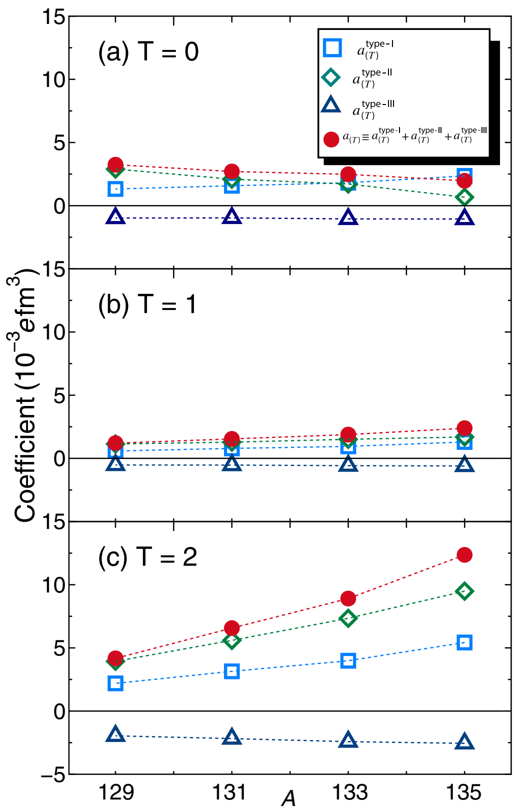

FIG. 3. The calculated results of $a_{(T)}$ for (a) $T = 0$, (b) $T = 1$, and (c) $T = 2$ as functions of mass number A for Xe isotopes (in units of 10^{-3} $e$fm^3). The squares, diamonds, triangles, and circles represent $a_{(T)}^{\text{type-I}}$, $a_{(T)}^{\text{type-II}}$, $a_{(T)}^{\text{type-II}}$, and $a_{(T)}$, respectively.

isoscalar component for ^{129}Xe becomes 6.4 times larger than the previous one. The reason for this difference between the present and previous results is discussed in Sec. IV.

The present results for Xe isotopes are summarized in Fig. 3. The calculated results of $a_{(T)}$ are shown for each isospin as functions of mass number A. Each $a_{(T)}$ smoothly decreases from ^{129}Xe to ^{135}Xe for the isoscalar ($T = 0$) component while it smoothly increases for the isovector ($T = 1$) and isotensor ($T = 2$) components.

IV. DISCUSSIONS

A. Comparison with other results

The present results, our previous results [27] and results by Dmitriev *et al.* [25] are compared for ^{129}Xe in Table V. The difference between the present study and the previous one is due to improvement of the model space adopted in the calculation.

In the previous study the model space for diagonalization was two major shells between the magic numbers 50 and 126. The Schiff moment was exactly calculated within this model space, but only four orbitals ($1f_{7/2}$, $2p_{3/2}$, $1f_{5/2}$, and $2p_{1/2}$) for type-I $1p1h$ excitations were assumed without considering type-II and type-III excitations.

In the present study the model space is limited only to the one major shell between the magic numbers 50 and 82. However, evaluation of the Schiff moment is carried out by taking all the $1p1h$ excitations not only to all the orbitals over 82, but also from all the orbitals under 50. Following the present framework, the Schiff moment is again evaluated using only the same orbitals and the same single-particle energies adopted in the previous study. Then $S = 0.84\bar{g}^{(0)}g + 0.36\bar{g}^{(1)}g + 1.32\bar{g}^{(2)}g$ (in units of 10^{-3} $e$fm^3) is obtained, which is reasonable compared with the previous result.

The Schiff moment of ^{129}Xe was also calculated by Dmitriev *et al.* [25]. They estimated the Schiff moment assuming that ^{129}Xe consists of the even-even core and one odd neutron. They calculated the Schiff moment and predicted the Schiff moment of ^{129}Xe with core polarization as $S = 8\bar{g}^{(0)}g + 6\bar{g}^{(1)}g - 9\bar{g}^{(2)}g$ (in units of 10^{-3} $e$fm^3), which more or less resembles our results. Note that our definition of the isotensor interaction in Eq. (8) is different in its sign from that of Ref. [25].

TABLE V. The comparison of $a_{(T)}$'s for ^{129}Xe between present results (This work), the results by Dmitriev *et al.* [25], and our previous results [27] in units of 10^{-3} $e$fm^3. The isotensor ($T = 2$) component in [25] is changed from its original sign in accordance with the different sign definition of the isotensor ($T = 2$) interaction in the present study.

T	This work	Ref. [25]	Ref. [27]
0	+3.242	+8	+0.507
1	+1.204	+6	+0.399
2	+4.172	+9	+1.89

B. Strength functions for the Schiff moment operator

To investigate each $1p1h$ contribution to the Schiff moment, the strength function for the Schiff moment operator defined by

$$s_{ph}(E_{ph}) = \sum_K \langle I_1^+ | S_0^{(1)} | (ph)K; I^- \rangle \tag{30}$$

and the strength function for the $V_{\pi(T)}^{PT}$ operator defined by

$$v_{ph(T)}^{PT}(E_{ph}) = \sum_K \langle (ph)K; I^- | V_{\pi(T)}^{PT} | I_1^+ \rangle \tag{31}$$

are both calculated and shown in Fig. 4 as a function of the energy denominator E_{ph} for the isoscalar ($T = 0$) components of ^{129}Xe. Here, partial contributions to the Schiff moment are also shown in Fig. 4, which is defined as

$$S_{ph(T)}(E_{ph}) = -\sum_K \frac{\langle I_1^+ | S_0^{(1)} | (ph)K; I^- \rangle \langle (ph)K; I^- | V_{\pi(T)}^{PT} | I_1^+ \rangle}{E_{ph}} + \text{c.c.} \tag{32}$$

The Schiff moment strengths are large both in regions between $5 \sim 15$ MeV and between $25 \sim 35$ MeV [see Fig. 4(a)]. In contrast, the $V_{\pi(T)}^{PT}$ strength has several large contributions in the region between $5 \sim 15$ MeV, but not so large contributions above 25 MeV [see Fig. 4(b)]. As seen in Fig. 4(c), initially the sign of the Schiff moment is negative due to the first

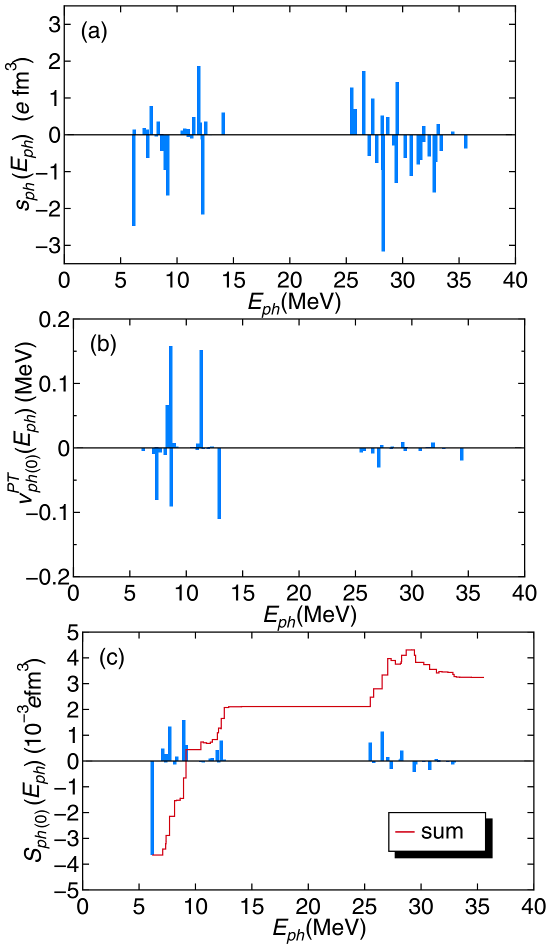

FIG. 4. (a) The strength functions of Schiff moment operator as a function of the energy denominator E_{ph} for isoscalar ($T = 0$) contributions of ^{129}Xe. (b) The same as in (b), but for $V^{PT}_{\pi(T)}$ operator. (c) The same as in (a), but for partial contribution to the Schiff moment. The summation of partial contributions to the Schiff moment is also shown.

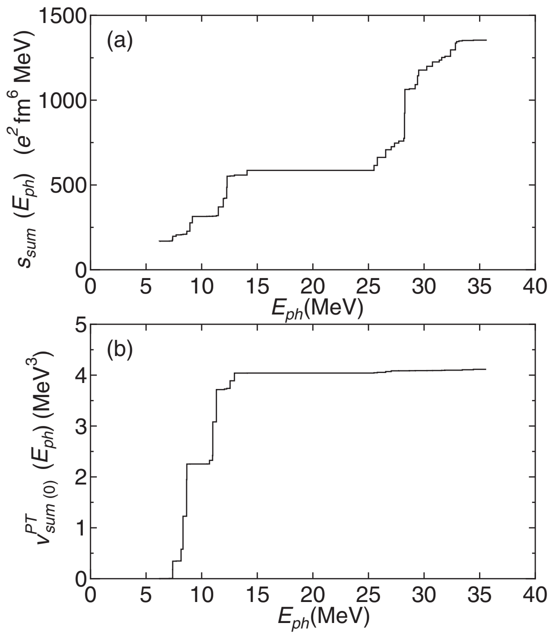

FIG. 5. (a) Energy weighted sum function for the Schiff moment operator as a function of the energy denominator E_{ph} for ^{129}Xe. (b) The same as in (a), but for $V^{PT}_{\pi(T)}$ operator with the isoscalar ($T = 0$) component.

large negative contributions at around 6 MeV. However, most of partial contributions to the Schiff moment after the large negative contribution are positive. Then the value of the Schiff moment gradually goes up to zero and finally the sign of the Schiff moment becomes positive. The value of the total Schiff moment is mostly determined by the energy of 15 MeV and there are only limited contributions above 25 MeV. It is noted that the energy difference of 15 $\sim$ 25 MeV exactly corresponds to the energy gap of 2 $\hbar\omega$ and these states in the gap are not connected by the Schiff moment operator from the $|I_1^+\rangle$.

In order to check the sum rule for the Schiff moment operator, we define the following energy-weighted function:

$$s_{\rm sum}(E_{ph}) \equiv \sum_{E=E_0}^{E_{ph}} E|S_{ph}(E)|^2, \tag{33}$$

where E_0 is the ground-state energy. Then the Thomas-Reiche-Kuhn (TRK) sum S_{EW} [40–42] becomes

$$S_{EW} = \lim_{E_{ph}\to\infty} s_{\rm sum}(E_{ph}) = \tfrac{1}{2}\langle I_1^+|[[S_0^{(1)}, H_0], S_0^{(1)}]|I_1^+\rangle. \tag{34}$$

Recently the right-hand side of Eq. (34) is evaluated using the random phase approximation (RPA) formalism [43] in the atomic systems.

We also define a similar energy-weighted function for the PT-violating potential,

$$V^{PT}_{\rm sum(0)}(E_{ph}) \equiv \sum_{E=E_0}^{E_{ph}} E|v_{ph(0)}(E)|^2, \tag{35}$$

where the subscript 0 indicates the isoscalar potential with $T = 0$. These functions are shown in Fig. 5. The figures show that, although the squared strength of the Schiff operator is distributed even up to the particle-hole energy of 33 MeV, that of the PT-violating potential already becomes very small after the energy of 13 MeV.

C. Effects of residual interactions

Now let us discuss the effects of residual interactions. In the mean field theories it is well known that the distributions of multipole operators have large collective peaks and that the residual interaction moves significant amounts of their strengths up or down [44]. Here the residual interaction means the remnant interaction of the two-body interaction, which is not taken into account in the mean field, namely, which is not absorbed in the one-body interaction. In the shell model approach two-body interactions are exactly diagonalized in the model space and there is no need to care about the residual interaction in the usual sense. However, even in the shell model approach the interaction among nucleons in the model space and those outside the model space has not been considered. Here we denote this interaction as the residual interaction in the shell model approach.

The unperturbed P and T conserving Hamiltonian H_0 consists of three parts: $H_0 = H_P + H_Q + H_{PQ}$. Here, H_P, H_Q, and H_{PQ} represent the interaction among nucleons in the model space, the interaction among nucleons outside the model space and the interaction among nucleons between the model space and the outside space, respectively. The detailed explanation is given in Appendix B. Up to now, effects of the residual interaction H_{PQ} and the two-body interaction in the model space $H_P^{(2)}$ have been neglected in the evaluation of Eq. (5).

The effects of the H_{PQ} and $H_P^{(2)}$ interactions appear in the energy denominator in Eq. (5). The expectation values of H_{PQ} and $H_P^{(2)}$ in terms of $1p1h$ states are denoted as ΔE_{PQ}^{ph} and ΔE_P^{ph}, where p and h represent particle and hole single-particle states, respectively.

Here, the effects due to the neglected interactions are estimated by varying the energy $\Delta E^{ph} = \Delta E_{PQ}^{ph} + \Delta E_P^{ph}$. The smallest single-particle excitation energy is found to be $E_{ph} = \varepsilon_p - \varepsilon_h = 6.2$ MeV (energy difference between the $0g_{9/2}$ and the $0h_{11/2}$ orbitals). Accordingly, the Schiff moment is evaluated by taking $\Delta E^{ph} = \pm 1$ MeV. Here it has been assumed that the ΔE^{ph} should not be large compared to E_{ph} so that ΔE^{ph} is set constant. In the case with $\Delta E^{ph} = +1$ MeV, the Schiff moment of ^{129}Xe is calculated as $S = 3.32\bar{g}^{(0)}g + 0.98\bar{g}^{(1)}g + 4.00\bar{g}^{(2)}g$ (in units of 10^{-3} $e$fm^3) and in the opposite case of $\Delta E^{ph} = -1$ MeV, the Schiff moment of ^{129}Xe is calculated as $S = 3.12\bar{g}^{(0)}g + 1.22\bar{g}^{(1)}g + 4.19\bar{g}^{(2)}g$ (in units of 10^{-3} $e$fm^3). The difference between results with and without ΔE^{ph} is about 10%.

D. Estimation of the atomic EDM and the global analysis

The relation between the Schiff moment and the atomic EDM of ^{129}Xe was calculated in Refs. [37–39]. Using the following relation [37]:

$$d(^{129}\mathrm{Xe}) = 0.38 \times 10^{-17}\left(\frac{S}{e\mathrm{fm}^3}\right)e\,\mathrm{cm}, \tag{36}$$

and the standard value of $g = 13.5$, the atomic EDM for ^{129}Xe is obtained as (in units of $10^{-19}e$ cm)

$$d(^{129}\mathrm{Xe}) = 1.66\bar{g}^{(0)} + 0.62\bar{g}^{(1)} + 2.14\bar{g}^{(2)}. \tag{37}$$

Now let us estimate the atomic EDM within the Standard Model. The strong πNN coupling constants $\bar{g}^{(T)}$ in the Standard Model are recently estimated by Yamanaka *et al.* [45]

$$\bar{g}^{(0)} = -1.1 \times 10^{-17}, \tag{38}$$

$$\bar{g}^{(1)} = -1.3 \times 10^{-17}, \tag{39}$$

$$\bar{g}^{(2)} = +3.3 \times 10^{-21}. \tag{40}$$

Using these values, the atomic EDM for ^{129}Xe in the Standard Model is estimated as

$$|d_{\mathrm{SM}}(^{129}\mathrm{Xe})| = 2.5 \times 10^{-36}e\,\mathrm{cm}. \tag{41}$$

If a larger EDM than that in Eq. (41) is observed in experiment, it becomes obvious evidence for physics beyond the Standard Model.

In Ref. [46], constraints on P and T violating hadronic and electron-nucleon parameters for diamagnetic systems and the neutron were obtained using experimental upper limits on EDMs and calculated Schiff moments for TlF molecule, ^{199}Hg, ^{129}Xe, and neutron. Similar analyses are performed by incorporating the Schiff moment of ^{129}Xe in the present work and also the EDM of ^{199}Hg in the update experiment [10],

$$|d(^{199}\mathrm{Hg})| < 7.4 \times 10^{-30}e\,\mathrm{cm}. \tag{42}$$

Table VI shows the results of constraints on P and T violating hadronic and electron-nucleon parameters for diamagnetic systems and the neutron. Each coefficient does not largely differ from the previous results [46], although all coefficients become slightly larger.

V. SUMMARY

In the present study the nuclear Schiff moments induced by the interaction which violates parity and time reversal invariance are calculated for the lowest $1/2^+$ states of Xe isotopes. The wave functions of Xe isotopes are calculated in terms of the nuclear shell model approach. Excitations from orbitals between the magic numbers 50 and 82 to orbitals over 82 (type-I excitations), the excitations from orbitals under 50 to orbitals between the magic numbers 50 and 82 (type-II

TABLE VI. P and T violating coefficients obtained from diamagnetic systems and the neutron. C_T is the tensor electron-nucleon couplings and $\bar{g}^{(T)}$ is the strong πNN constant which violates P and T invariance with isospin T. $\bar{d}_n^{sr}$ is a short-distance contribution to the neutron EDM. This work A (0.38) indicates that the factor 0.38 is used in Eq. (24), while the factor 0.27 is used for this work B (0.27) of Ref. [38], which is used in Ref. [46]. Compared to the analysis by [46] different signs are used for the coefficients in front of the $\bar{g}^{(0)}$ and $\bar{g}^{(1)}$. In the lowest row, the results in Ref. [46] are also shown.

	C_T	$\bar{g}^{(0)}$	$\bar{g}^{(1)}$	$\bar{d}_n^{sr}$ (e cm)
This work A (0.38)	2.208×10^7	-11.63×10^{-10}	1.710×10^{-10}	17.43×10^{-24}
This work B (0.27)	2.052×10^7	-10.82×10^{-10}	1.664×10^{-10}	16.20×10^{-24}
Ref. [46]	1.265×10^7	-6.687×10^{-10}	1.4308×10^{-10}	9.878×10^{-24}

excitations), and the excitations from orbitals under 50 to orbitals over 82 (type-III excitations) are considered for the one-particle and one-hole excitations. It is found that the contributions of type-II excitations are a few times larger than those from the type-I and type-III excitations. The contribution of excitation from the $0g_{9/2}$ orbital to the $0h_{11/2}$ orbital is the largest. It is also found that the excitations which require large excitation energies have negligible contributions.

The upper limit for the electric dipole moment of ^{129}Xe neutral atom is estimated using its Schiff moment. In the Standard Model it has been obtained as $|d_{\rm SM}(^{129}{\rm Xe})| = 2.5 \times 10^{-36} e\,$cm. If a much larger EDM is observed, it would be evidence for physics beyond the Standard Model.

It has been reported recently that the kaon exchange effect is sizable [45]. As a future work, this effect should be incorporated. Also it should be noted here that intrinsic EDMs of nucleons also contribute to the Schiff moments [27,28,47]. These contributions should be taken into account for more precise estimation of atomic EDMs.

ACKNOWLEDGMENTS

This work was supported by Grant-in-Aid for Scientific Research (C) No. 16K05341 and No. 25400267 from Japan Society for the Promotion of Science (JSPS), and also by Grant-in-Aid for JSPS Fellows Grant No. 2610429. The authors gratefully acknowledge fruitful discussions with Dr. N. Yamanaka and Dr. A. Umeya.

APPENDIX A

In the operator representation of the Rayleigh-Schrödinger perturbation theory with the unperturbed Hamiltonian H_0 and the perturbed Hamiltonian V:

$$H = H_0 + V, \tag{A1}$$

the ground state wave function is perturbed from $|\varphi_0\rangle$ to

$$|\psi_0\rangle = |\varphi_0\rangle + \frac{Q}{\varepsilon_0 - H_0} V|\varphi_0\rangle + \cdots . \tag{A2}$$

Here, $Q = 1 - P$ with $P = |\varphi_0\rangle\langle\varphi_0|$ and $H_0|\varphi_0\rangle = \varepsilon_0|\varphi_0\rangle$ with $|\varphi_0\rangle$ being normalized. Here, the deviation of normalization constant from one for $|\psi_0\rangle$ is due to second order of V and should be safely neglected in first order of V. Then the expectation value of the Schiff moment operator $S_0^{(1)}$ for the ground state $|\psi_0\rangle$ is expressed in first order of V as

$$\begin{aligned} S &= \langle\varphi_0|S_0^{(1)} \frac{Q}{\varepsilon_0 - H_0} V|\varphi_0\rangle + \text{c.c.} \\ &= \sum_{ij} \langle\varphi_0|S_0^{(1)}|i\rangle\langle i|\frac{1}{\varepsilon_0 - H_0}|k\rangle\langle k|QV|\varphi_0\rangle + \text{c.c.} \\ &= \sum_{ik} \frac{\langle\varphi_0|S_0^{(1)}|i\rangle\langle i|k\rangle\langle k|QV|\varphi_0\rangle}{\varepsilon_0 - \langle H_0\rangle_{ik}} + \text{c.c.} \\ &= \sum_{k} \frac{\langle\varphi_0|S_0^{(1)}|k\rangle\langle k|V|\varphi_0\rangle}{\varepsilon_0 - \langle H_0\rangle_{kk}} + \text{c.c.}, \end{aligned} \tag{A3}$$

where $\langle H_0\rangle_{kk} = \langle k|H_0|k\rangle$ and the complete relation of any basis states, $\sum |i\rangle\langle i| = \sum |k\rangle\langle k| = 1$ has been used. In the final expression both $\langle k|QV = \langle k|V$ and $\langle i|k\rangle = \delta_{ik}$ are assumed.

APPENDIX B

In the present paper the total Hamiltonian H is divided into the unperturbed part H_0 and the perturbation V as $H = H_0 + V$, where $H_0 = H_P + H_Q + H_{PQ}$ is the interaction which does not break P and T invariance and $V = V^{PT}$ is the P and T violating interaction.

In the following "c-particle" denotes any particle in an orbital between the magic numbers 50 and 82 and "a-particle" denotes any particle in an orbital over the magic number 82. Here, H_P is constructed solely from creation and annihilation operators of c-particles, H_Q is constructed solely by creation and annihilation operators of a-particles, and H_{PQ} is constructed by creation and annihilation operators of c- and a-particles. In the following only type-I excitations are considered for simplicity.

In order to avoid unnecessary complications, the angular momentum coupling and the single-particle orbital index are abbreviated. Let us consider the expectation value of $\langle H_0\rangle_{kk} = \langle k|H_0|k\rangle$, where $|k\rangle = a^\dagger c|\text{g.s.}\rangle$ is the $1p1h$ state constructed on the ground state $|\text{g.s.}\rangle$. Then we have

$$\begin{aligned} \langle k|H_0|k\rangle &= \langle \text{g.s.}|c^\dagger a H_0 a^\dagger c|\text{g.s.}\rangle \\ &= \langle \text{g.s.}|c^\dagger a\{[H_0,a^\dagger c] + a^\dagger c H_0\}|\text{g.s.}\rangle \\ &= E_{\text{g.s.}} + \langle \text{g.s.}|c^\dagger a[H_0,a^\dagger c]|\text{g.s.}\rangle \\ &= E_{\text{g.s.}} + \langle \text{g.s.}|[c^\dagger a,[H_0,a^\dagger c]]|\text{g.s.}\rangle. \end{aligned} \tag{B1}$$

Here, we have used the fact that the ground state $|\text{g.s.}\rangle$ consists only of c-particles. Namely $a|\text{g.s.}\rangle = 0$ and $H_0|\text{g.s.}\rangle = E_{\text{g.s.}}|\text{g.s.}\rangle$.

In the evaluation of the double commutator $[c^\dagger a,[H_0,a^\dagger c]]$, only the following terms in H_0 contribute to $\langle k|H_0|k\rangle$: (1) the term containing only one $a^\dagger$ and only one a operators, (2) the term containing neither $a^\dagger$ nor a operators.

Then up to two-body interactions, only the following Hamiltonians:

$$H_P = \varepsilon_c c^\dagger c + A c^\dagger c^\dagger c c, \tag{B2}$$

$$H_Q = \varepsilon_a a^\dagger a, \tag{B3}$$

$$H_{PQ}^{(2)} = J a^\dagger c^\dagger a c, \tag{B4}$$

contribute to $\langle k|H_0|k\rangle$, where A and J indicate strengths of two-body interactions depending on the orbitals involved. ε_c and ε_a indicate single-particle energies.

Finally, we have

$$\langle k|H_0|k\rangle = E_{\text{g.s.}} + \varepsilon_a - \varepsilon_c + \Delta E_P^{ac} + \Delta E_{PQ}^{ac}, \tag{B5}$$

where $\Delta E_P^{ac} \equiv \langle k|H_P^{(2)}|k\rangle$ and $\Delta E_{PQ}^{ac} \equiv \langle k|H_{PQ}^{(2)}|k\rangle$. Here, $H_P^{(2)} = A c^\dagger c^\dagger c c$ is the two-body part of the interaction H_P in the model space. $H_{PQ}^{(2)}$ corresponds to the residual interaction. The energy denominator in Eq. (A3) is given as (i.e., $\varepsilon_0 =$

$E_{\mathrm{g.s.}}$)

$$\varepsilon_0 - \langle H_0\rangle_{kk} = \varepsilon_c - \varepsilon_a - \Delta E_P^{ac} - \Delta E_{PQ}^{ac}. \tag{B6}$$

APPENDIX C

In order to evaluate Eq. (5), intermediate states

$$|(ph)K;I^-\rangle = N_{ph}^{(K)}[[a_p^\dagger \tilde{c}_h]^{(K)} \otimes |I_1^+\rangle]^{(I)} \tag{C1}$$

should form an orthonormal system. In principal each state is orthonormalized by Schmidt orthogonalization procedure by requiring

$$\langle (p'h')K';I^-|(ph)K;I^-\rangle = \delta_{p'p}\delta_{h'h}\delta_{K'K}. \tag{C2}$$

Since it is a hard task to accomplish this requirement numerically, for the type-I excitations, e.g., we only require

$$\langle (ph)K;I^-|(ph)K;I^-\rangle = 1 \tag{C3}$$

and

$$\langle (p'h)K';I^-|(ph)K;I^-\rangle = \delta_{p'p}\delta_{K'K}. \tag{C4}$$

Thus

$$\langle (ph')K;I^-|(ph)K;I^-\rangle = \delta_{h'h} \tag{C5}$$

is only approximately realized in this work. This overlap is non-zero only when both h' and h single-particle states are occupied in $|I_1^+\rangle$. Thus this overlap is expected to be very small in a many-body system.

[1] M. Kobayashi and T. Maskawa, Prog. Theor. Phys. **49**, 652 (1973).
[2] C. A. Baker *et al.*, Phys. Rev. Lett. **97**, 131801 (2006).
[3] M. B. Gavela, A. Le Yaouanc, L. Oliver, O. Pene, J.-C. RaynaL, and T. N. Pham, Phys. Lett. B **109**, 215 (1982).
[4] I. B. Khriplovich and A. R. Zhitnitsky, Phys. Lett. B **109**, 490 (1982).
[5] M. Pospelov and A. Ritz, Ann. Phys. (NY) **318**, 119 (2005).
[6] J. M. Pendlebury and E. A. Hinds, Nucl. Instrum. Methods Phys. Res. A **440**, 471 (2000).
[7] J. Engel, M. J. Ramsey-Musolf, and U. van Kolck, Prog. Part. Nucl. Phys. **71**, 21 (2013).
[8] T. Fukuyama, Int. J. Mod. Phys. A **27**, 1230015 (2012).
[9] M. A. Rosenberry and T. E. Chupp, Phys. Rev. Lett. **86**, 22 (2001).
[10] B. Graner, Y. Chen, E. G. Lindahl, and B. R. Heckel, Phys. Rev. Lett. **116**, 161601 (2016).
[11] R. H. Parker, M. R. Dietrich, M. R. Kalita, N. D. Lemke, K. G. Bailey, M. Bishof, J. P. Greene, R. J. Holt, W. Korsch, Z.-T. Lu, P. Mueller, T. P. O'Connor, and J. T. Singh, Phys. Rev. Lett. **114**, 233002 (2015).
[12] A. Yoshimi, T. Inoue, T. Furukawa, T. Nanao, K. Suzuki, M. Chikamori, M. Tsuchiya, H. Hayashi, M. Uchida, N. Hatakeyama, S. Kagami, Y. Ichikawa, H. Miyatake, and K. Asahi, Phys. Lett. A **376**, 1924 (2012).
[13] W. Heil *et al.*, Ann. Phys. (Berlin) **525**, 539 (2013).
[14] M. D. Swallows, T. H. Loftus, W. C. Griffith, B. R. Heckel, E. N. Fortson, and M. V. Romalis, Phys. Rev. A **87**, 012102 (2013).
[15] E. R. Tardiff *et al.*, Phys. Rev. C **77**, 052501(R) (2008).
[16] Y. F. Orlov, W. M. Morse, and Y. K. Semertzidis, Phys. Rev. Lett. **96**, 214802 (2006).
[17] S. Oshima, Phys. Rev. C **81**, 038501 (2010).
[18] C. Itoi and S. Oshima, J. Phys. Soc. Jpn. **79**, 103201 (2010).
[19] N. Yamanaka and E. Hiyama, Phys. Rev. C **91**, 054005 (2015).
[20] J. Engel, M. Bender, J. Dobaczewski, J. H. de Jesus, and P. Olbratowski, Phys. Rev. C **68**, 025501 (2003).
[21] J. H. de Jesus and J. Engel, Phys. Rev. C **72**, 045503 (2005).
[22] J. Dobaczewski and J. Engel, Phys. Rev. Lett. **94**, 232502 (2005).
[23] N. Auerbach, V. F. Dmitriev, V. V. Flambaum, A. Lisetskiy, R. A. Sen'kov, and V. G. Zelevinsky, Phys. Rev. C **74**, 025502 (2006).
[24] S. Ban, J. Dobaczewski, J. Engel, and A. Shukla, Phys. Rev. C **82**, 015501 (2010).
[25] V. F. Dmitriev, R. A. Sen'kov, and N. Auerbach, Phys. Rev. C **71**, 035501 (2005).
[26] N. Yoshinaga, K. Higashiyama, and R. Arai, Prog. Theor. Phys. **124**, 1115 (2010).
[27] N. Yoshinaga, K. Higashiyama, R. Arai, and E. Teruya, Phys. Rev. C **87**, 044332 (2013); **89**, 069902(E) (2014).
[28] N. Yoshinaga, K. Higashiyama, R. Arai, and E. Teruya, Phys. Rev. C **89**, 045501 (2014).
[29] R. A. Sen'kov, N. Auerbach, V. V. Flambaum, and V. G. Zelevinsky, Phys. Rev. A **77**, 014101 (2008).
[30] W. C. Haxton and E. M. Henley, Phys. Rev. Lett. **51**, 1937 (1983).
[31] P. Herczeg, Hyperfine Interact. **43**, 75 (1988).
[32] P. Herczeg, Hyperfine Interact. **75**, 125 (1992).
[33] K. Higashiyama, N. Yoshinaga, and K. Tanabe, Phys. Rev. C **67**, 044305 (2003).
[34] N. Yoshinaga and K. Higashiyama, Phys. Rev. C **69**, 054309 (2004).
[35] K. Higashiyama and N. Yoshinaga, Phys. Rev. C **83**, 034321 (2011); **89**, 049903(E) (2014).
[36] C. Gustafson, I. L. Lamm, B. Nilsson, and S. G. Nilsson, Arkiv Fysik **36**, 613 (1967).
[37] V. A. Dzuba, V. V. Flambaum, and P. G. Silvestrov, Phys. Lett. B **154**, 93 (1985).
[38] V. A. Dzuba, V. V. Flambaum, J. S. M. Ginges, and M. G. Kozlov, Phys. Rev. A **66**, 012111 (2002).
[39] Y. Singh, B. K. Sahoo, and B. P. Das, Phys. Rev. A **89**, 030502(R) (2014); **90**, 039903(E) (2014).

[40] W. Thomas, Naturwissenschaften **13**, 627 (1925).
[41] W. Kuhn, Z. Phys. **33**, 408 (1925).
[42] F. Reiche and W. Thomas, Z. Phys. **34**, 510 (1925).
[43] https://arxiv.org/abs/0906.2911.
[44] N. Auerbach, J. Phys.: Conf. Series **724**, 012002 (2016), and references therein.
[45] N. Yamanaka and E. Hiyama, J. High Energy Phys. 02 (2016) 067.
[46] T. Chupp and M. Ramsey-Musolf, Phys. Rev. C **91**, 035502 (2015).
[47] V. F. Dmitriev and R. A. Sen'kov, Phys. Rev. Lett. **91**, 212303 (2003).